RESEARCH ARTICLE

Influence of Surface Modification on Corrosion Behavior of the Implant Grade Titanium Alloy Ti-6Al-4V, in Simulated Body Fluid: An *In Vitro* Study

Vizaikumar Vasudha Nelluri[1], Rajani Kumar Gedela[2], Maria Roseme Kandathilparambil[3]

Abstract

Aim and objective: To evaluate the influence of surface modification on corrosion behavior of the implant grade titanium alloy Ti-6Al-4V, in simulated body fluids (SBFs).

Materials and methods: Seventy disk-shaped samples of implant grade titanium alloy, Ti-6Al-4V were divided into seven groups of 10 each; UMS (unmodified surface/control group), HA (hydroxyapatite coated), LS (LASER sintered), LT (LASER textured), TG (combined chemical and thermal treated), HT850 (oxidized state), and HT1050 (oxidized state) were subjected to corrosion tests, electrochemical impedance, and cyclic polarization tests using GAMRY Potentiostat in SBF. Paired *t*-test, one-way analysis of variance (ANOVA) test, and Tukey honestly significant difference (HSD) test ($p = 0.05$).

Results: Polarization resistance (R_p) was increased in TG (1,800 ± 10.54 kΩ) with respect to UMS (control group) (1,249 ± 11.25 kΩ) and HA (1,250 ± 8.65 kΩ), further reduced in HT850 (780.00 ± 11.54 kΩ), LT (127 ± 5.37 kΩ), LS (60 ± 18.26 kΩ), and HT1050 (0.00 ± 0.00 kΩ) being lowest at 144 hours. Their mean comparisons were statistically significant except in HT1050 ($p = 0.05$). Cyclic polarization curves showed hysteresis loops in all the samples (UMS, HA, LS, LT, HT850, and HT1050) indicating susceptibility to localized corrosion (pitting and crevice corrosion) except in the TG sample, which showed forward scan retracing the reverse scan; they showed significantly improved resistance against pitting in TG followed by LS, HA, LT, and HT850 compared to UMS (control) except HT1050 ($p = 0.05$).

Conclusion: Combined chemical and thermal treatment of titanium alloy showed greater corrosion resistance and minimal susceptibility to localized corrosion (pitting and crevice corrosion) than the unmodified surface.

Keywords: Corrosion, Hydroxyapatite, LASER sintered, LASER textured, Surface modification, Ti-6Al-4V.

International Journal of Prosthodontics and Restorative Dentistry (2020): 10.5005/jp-journals-10019-1280

Introduction

Metallic biomaterials, such as, 316L stainless steel, cobalt-chromium-molybdenum, pure titanium, and titanium-based alloys, are commonly used as orthopedic and dental implants. Biomaterials are commonly defined as non-viable materials intended to interact with biological systems to evaluate, treat, augment, or replace any tissue, organ, or function of the body.[1] Biocompatibility is an essential requirement of a biomaterial. A biocompatible material performs an appropriate host response (i.e., minimum disruption of normal body function) in a specific application.[2] It implies that the material should not cause any toxic or inflammatory reaction when placed in the human body. The factors that determine the biocompatibility are, the host reactions induced by the material and the degradation/corrosion of the material in the body/oral environment.

Commercially pure titanium (CP-Ti) and its alloys are mostly used as medical implants.[3] They are corrosion resistant due to the formation of a protective oxide layer on its surface, thus preventing corrosion. Consequently, the release of ionic or by-product residue into the periprosthetic tissue is minimal and these biomaterials may be classified as biologically inert or electrochemically passive in the whole range of clinically relevant potential-pH combinations.[4] Ti-alloys with their excellent chemical and mechanical properties and biocompatibility are a suitable choice for implant applications, thus reducing the utilization of rare metals. These alloys have become the structural materials for replacing hard human tissue. Among the other mechanical properties, the low Young's modulus of these alloys avoids the occurrence of stress shielding after implantation.[5]

Although the CP-Ti and Ti-6Al-4V alloys exhibit excellent resistance against general and pitting corrosion, the low wear

[1]Department of Prosthodontics, Maxillofacial Prosthesis and Implantology, Government Dental College and Hospital, Afzalgunj, Hyderabad, Telangana, India

[2]Department of Periodontics, Army College of Dental Sciences, Jai Jawahar Nagar, Secunderabad, Telangana, India

[3]Department of Prosthodontics, SB Patil Dental College and Hospital, Bidar, Karnataka, India

Corresponding Author: Vizaikumar Vasudha Nelluri, Department of Prosthodontics, Maxillofacial Prosthesis and Implantology, Government Dental College and Hospital, Afzalgunj, Hyderabad, Telangana, India, Phone: +91 8074358918, e-mail: nvasudha@yahoo.com

How to cite this article: Nelluri VV, Gedela RK, Kandathilparambil MR. Influence of Surface Modification on Corrosion Behavior of the Implant Grade Titanium Alloy Ti-6Al-4V, in Simulated Body Fluid: An *In Vitro* Study. Int J Prosthodont Restor Dent 2020;10(3):102–111.

Source of support: Nil

Conflict of interest: None

resistance and the possibility of vanadium release from Ti-6Al-4V may induce aseptic loosening during long-term implantation.[6,7] Even though Ti-6Al-4V releases undesirable vanadium, the formation of a uniform, adherent TiO_2 film, makes it a choice for bioapplications. Ti-6Al-4V is modified by replacing V with Nb, Zr, or Ta to make it more biocompatible and corrosion-resistant. Another approach adopted was surface modifications, such as, laser (laser surface melting and laser surface alloying), electrochemical oxidation, and thermal oxidation techniques to enhance the corrosion resistance and biocompatibility.[8] Also, modification of the surface of the dental implants by changing the roughness and porosity of the surface is known to enhance the process of osseointegration,[9–16] which is considered to be crucial for ideal prosthetic fixation.

On implantation, body temperature remains 37°C, but pH drops from 7.4 to 4.00 due to the formation of hematoma around the implants.[17] Intraorally, exposed parts of the implant come in contact with highly acidic food and fluorides of dental products that are corrosive. Hence, there is a need to assess the biocompatibility of an implant material as such and with surface modifications, thus enabling us to understand the degradation/corrosion of the material in the body/oral environment on long-standing.

Corrosion behavior of dental alloys is assessed in simulated body fluid (SBF) using different techniques, such as, potentiostatic, anodic polarization, and impedance spectroscopy for characterization of corrosion.[18–22] Various solutions like artificial saliva, Ringer's solution, and SBF have been used[23–26] as corrosive media to simulate the conditions encountered inside the body.

The main objectives of the present study are to improve the surface area of implant grade Ti-6Al-4V alloy by modifying its surface through hydroxyapatite coating, surface texturing, and sintering with TiO_2 using LASER, a combination of chemical and thermal treatments, and surface oxidation treatments; evaluate their corrosion resistance which governs the biocompatibility and durability of the modified surfaces by subjecting them to corrosion tests namely, electrochemical impedance and cyclic polarization tests (CPTs) in SBF. The null hypothesis being that the different surface modifications of implant grade Ti-6Al-4V alloy surfaces do not influence its corrosion behavior.

The present investigation is concerned with the study of the influence of surface modifications of the implant grade titanium alloy, Ti-6Al-4V, on its *in vitro* biocompatibility through electrochemical impedance spectroscopy (EIS) and CPTs in SBF at 37°C.

Materials and Methods

Materials

The surgical/implant grade alloy Ti-6Al-4V was procured in the form of cylindrical rods of 20 mm diameter from M/S Mishra Dhatu Nigam Limited (MIDHANI), Hyderabad, Telangana State, India conforming to ASTM, BSI, and ISO specifications (ISO: 5832-3; 1996. Implants for Surgery, Metallic Parts—Part 3).[27]

Methodology

An experimental *in vitro* study was performed according to the study design as described in the Flowchart 1.

Sample Preparation

Seventy disk-shaped samples of 5 mm thickness and 20 mm diameter were prepared by transverse sectioning of the Ti-6Al-4V

Flowchart 1: Flowchart showing the study design; UMS (unmodified surface/control group), HA (hydroxyapatite coated), LS (LASER sintered), LT (LASER textured), TG (combined chemical and thermal treated), HT850 (oxidized state), and HT1050 (oxidized state)

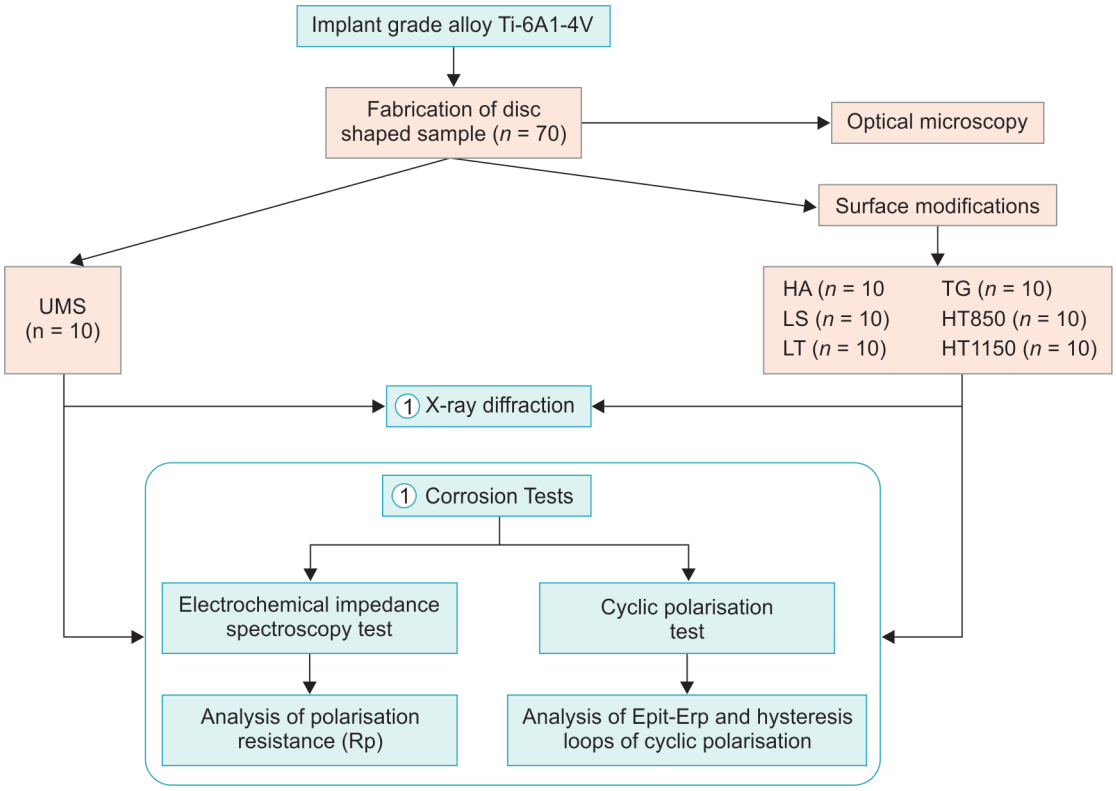

alloy rod. All the samples were mechanically polished from 1/0 to 4/0 emery paper, ultrasonically cleaned for 15 minutes in acetone and 15 minutes in distilled water. They were divided into seven groups of 10 each, namely UMS (unmodified surface/control group), HA (hydroxyapatite coated), LS (LASER sintered), LT (LASER textured), TG (combined chemical and thermal treated), HT850 (oxidized state), and HT1050 (oxidized state). One side of the two flat surfaces of the sample disks was subjected to surface modification and the flat surface of the other side as well as the circumferential surface of 5 mm thickness was covered with lacquer.

Surface Treatment Procedure of Each Group

The surface modification treatments included in the present study, namely hydroxyapatite coating, LASER sintering, and LASER texturing were carried out at the International Advanced Research Centre for Powder Metallurgy and New Materials (ARCI), Hyderabad, Telangana State, India. Other surface modification treatments, namely a combination of chemical and thermal treatments, and surface oxidation treatments (Fig. 1) were carried out at the Department of Metallurgical Engineering, Information Technology, Banaras Hindu University, Varanasi, India. The description of the surface modifications carried in each group is described as follows.

UMS (unmodified surface/control group, 10 samples): The disks were mechanically polished from 1/0 to 4/0 emery paper, ultrasonically cleaned for 15 minutes in acetone and 15 minutes in distilled water.

HA (hydroxyapatite coated, 10 samples): The polished and cleaned disks were sprayed with hydroxyapatite particles (hydroxyapatite powder, Himed, New York, USA), using detonation gun technique (detonation spraying equipment, Plakart D-3, Moscow) resulting in the chemically stable adhesion of hydroxyapatite coating.

LS (LASER sintered, 10 samples): Titanium alloy powdered particles were sintered/alloyed on the surface of disks samples using LASER (JK704 model pulsed Nd:YAG LASER equipment) with the energy of 6.7 J, pulse duration of 5.2 ms, frequency of 44 Hz, and power of 300 W in a chamber maintained at a pressure of 4 bar of Ar.

LT (LASER textured, 10 samples): Texturing was done by melting the surface of the disks samples with LASER (JK704 model pulsed Nd:YAG LASER equipment) with the energy of 6.7 J, pulse duration of 5.2 ms, frequency of 44 Hz, and power of 300 W in a chamber maintained at a pressure of 4 bar of Ar.

TG (combined chemical and thermal treated, 10 samples): A layer of thin and adherent bioactive titania gel is grown on the surface of the base material by giving a combined chemical and thermal treatment. This treatment consisted of soaking of the sample in a 6% (by mass) hydrogen peroxide solution at 60°C for 4 hours and subsequent heating at 400°C for 1 hour, followed by furnace cooling.

HT850 (oxidized state, 10 samples): Surface oxidation treatment was carried out at a temperature of 850°C for 1 hour in the air.

HT1050 (oxidized state, 10 samples): Surface oxidation treatment was carried out at temperatures of 1,050°C for 1 hour in the air.

X-ray Diffraction Analysis

X-ray diffraction (XRD) analysis was carried out (D8 advance BRUKER) to characterize the various phases present in the samples after different surface modifications. Cu-Kα radiation of wavelength 1.5402 Å with Ni filter was used.

Corrosion Tests

Corrosion tests were carried out in a glass cell (200 mL) containing SBF, prepared by dissolving reagent-grade NaCl, $NaHCO_3$, KCl, K_2HPO_4, $MgCl_2{\cdot}6H_2O$, $CaCl_2$, and Na_2SO_4 in distilled water buffered at pH 7.4 at 37°C with 50 mM tris-hydroxymethyl-aminomethane $(CH_2OH)_3CNH_2$ and 45 mM hydrochloric acid. The expected concentration of various ions in mM were 142 Na^+, 5 K^+, 1.5 Mg^{2+}, 2.5 Ca^{2+}, 147.8 Cl^-, 4.2 HCO^{3-},1 HPO_4^{2-}, and 0.5 SO_4^{2-}. The solution was kept at a constant temperature of 37°C. Electrochemical impedance spectroscopy test and CPT were carried for all the samples using GAMRY Potentiostat (PC4 Series, Gamry Instruments, 734 Louis Drive, Warminster, Pennsylvania 18974, USA). All the experiments were performed by the defined instructions by ASTM standards.[28] All 10 samples of each group were tested.

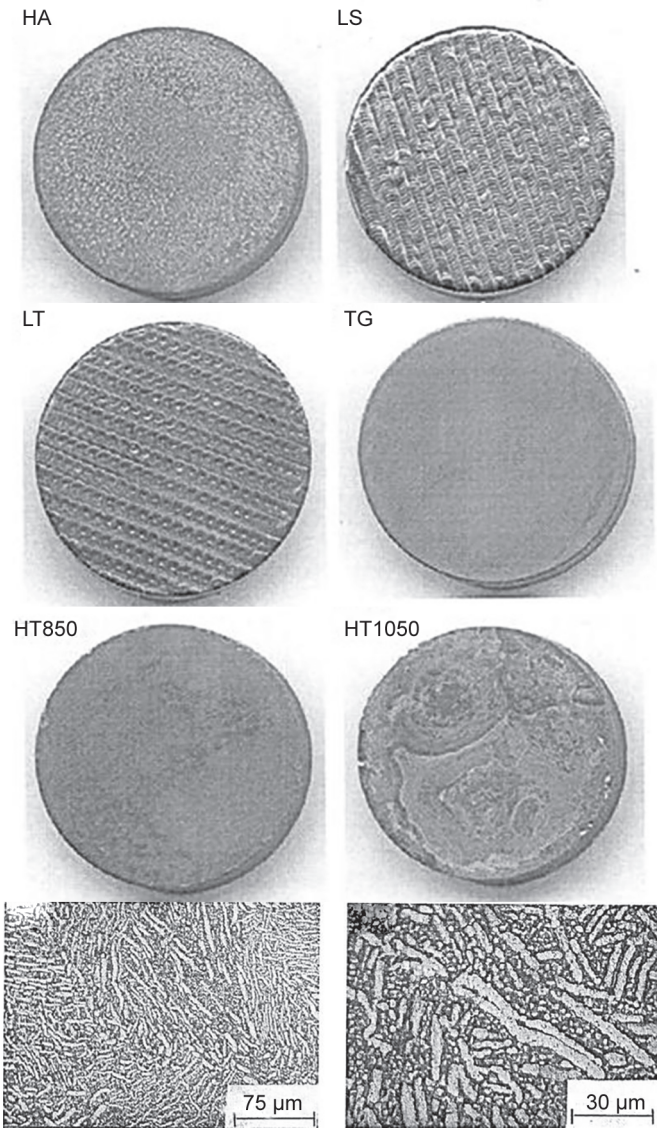

Fig. 1: Surface modification of groups—UMS (unmodified surface), HA (hydroxyapatite coated), LS (LASER sintered), LT (LASER textured), TG (combined chemical and thermal treated), HT850 (oxidized state), and HT1050 (oxidized state); optical micrographs of the alloy Ti-6Al-4V at different magnifications- 75 µm and 30 µm

EIS Test

The electrochemical impedance spectra were obtained by using a frequency response analyzer (Echemst Analyst) connected to a GAMRY Potentiostat. Electrochemical impedance/alternating current (AC) impedance test was carried out as after imposing an ac signal of amplitude 10 mV of sinusoidal voltage at open circuit potential of the samples, in the frequency domain analyzed ranged from 10 Hz to 100 kHz. Conventional three electrodes were used as reference saturated calomel electrodes, a graphite rod as a counter electrode, and the test sample as a working electrode.

An impedance method is a straightforward approach for analyzing electrical circuits and extracting the values of three circuit parameters namely polarization resistance (R_p), solution resistance (Rs), and double-layer capacitance (Cdl) that approximate a corroding electrochemical interface.[29] The EIS data were recorded according to the defined ASTM standards (G 106).[30]

CPT

The CPT was conducted in the range of −1.000 to 2.000 mV (saturated calomel electrode = SCE) concerning the open circuit potential. All the groups were subjected to CPT and curves were recorded at a scan rate of 0.2 mV/s. Anodic and cathodic corrosion potentials were recorded as volt vs SCE plot for various current densities at room temperature. The samples were immersed for 15 minutes in the electrolyte before starting the polarization scan at −1.000 mV. The scan was initiated in a more noble direction at a scan rate of 0.2 mV/s. When 1,500 mV was reached, the scanning direction was reversed. The scan was terminated when the potential reverted, once again to −1.000 mV. To assess the corrosion susceptibility of small implant devices and localized corrosion, susceptibility measurements are recorded according to the defined ASTM standards (F2129, G61).[31,32] The corrosion current density (i_{corr}), corrosion potential (E_{corr}), pitting potential (E_{pit}), repassivation or protection potential (E_{rep}), and hysteresis of each specimen were determined from polarization curves. The polarization curves [potential (*v*) is plotted against current density in a/cm^2] are shown in Figure 2.

Statistical Analysis

All the obtained data were entered into IBM SPSS Statistics 22.0 version software. Paired *t*-test, one-way analysis of variance

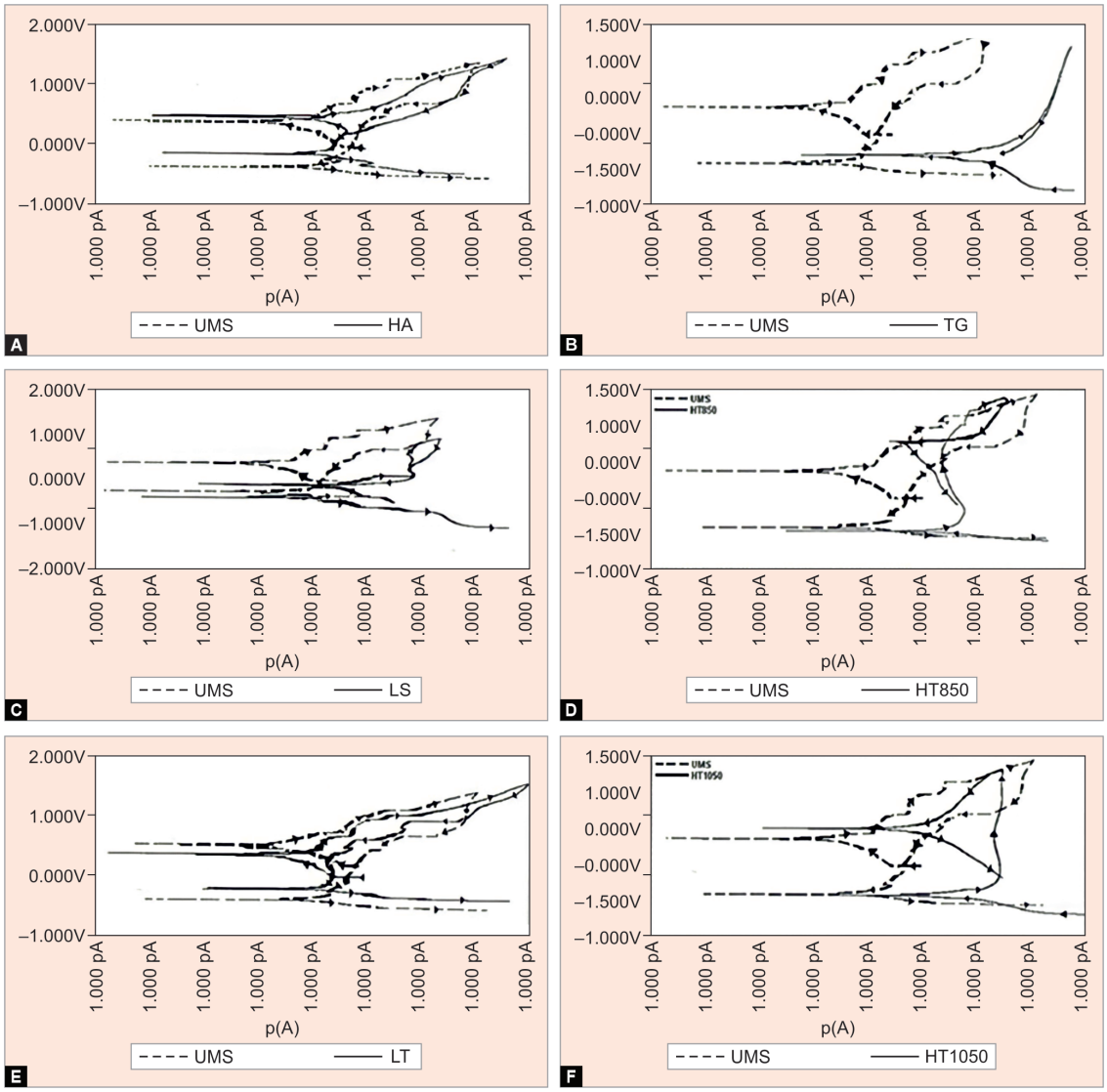

Figs 2A to F: Cyclic polarization scans for HA (A), LS (B), LT (C), TG (D), HT850 (E), and HT1050 (F); surface-modified conditions plotted along with the unmodified condition (UMS) and the arrows indicate the direction of polarization

(ANOVA) test, and Tukey honestly significant difference (HSD) test were performed with a *p* value of 0.05.

Results

Microstructure Characterization

A study of the microstructure of the alloy Ti-6Al-4V was carried out by optical microscopy and the optical micrograph showed dual-phase microstructure consisting of mainly α (the light etching phase), in the matrix of β (the dark phase) as shown in Figure 1. Thus, it reveals that the samples consist of mainly fine-grained hcp (α) phase distributed in the bcc (β) phase indicating higher strength and corrosion resistance.

XRD Analysis

X-ray diffraction patterns of the unmodified surface (UMS) Ti-6Al-4V alloy with different surface modifications are shown in Figure 3. Surface modifications of implant grade titanium alloy Ti-6Al-4V developed various oxides and phases on its surface, such as, hydroxyapatite coated (HA)—non-crystalline; LASER sintered (LS)—TiO_2 (titania) and Al_2O_3 (alumina); LASER textured (LT)—TiO_2, Al_2O_3, TiO_3, and V_2O; combined chemical thermal treated (TG)—TiO_2; oxidized state (HT850)—TiO_2, Ti_2O_3, Ti_3O_5, V_6O_{13}, and $AlTi_3$; oxidized state (HT1050)—TiO_2, Al_2O_3, Ti_3O_5, V_2O_5, VO_2, and $Al_{23}O_4$; and UMS (unmodified surface/control group) surface consisted TiO_2 and Al_2O_3.

It may be seen that while there is only the presence of TiO_2 in the TG sample, there is TiO_2 as well as Al_2O_3 in the LS condition. The other surface-modified samples like LT, HT850, and HT1050 may be seen to contain many other oxides of Vanadium and phases in addition to those of alumina and titania.

Corrosion Behavior

The electrochemical impedance spectroscopic (EIS) data were recorded and a mean comparison of R_p between 24 hours and 144 hours duration of exposure in SBF solution of all study groups with various surface modifications is shown in Table 1. The paired *t*-test for mean comparison of R_p between 24 hours and 144 hours duration of the groups UMS, HA, LS, LT, TG, and HT850 in the study showed statistically significant difference ($p = 0.05$) except HT1050. It indicates that the surface modifications namely UMS, HA, LS, LT, TG, and HT850 have a significant influence on the corrosion resistance but have no observed influence in HT1050. One-way ANOVA test for 24 and 144 hours within the groups using mean comparisons of R_p showed that all the modifications had a significant difference in corrosion resistance.

It may be seen that R_p of the alloy Ti-6Al-4V is markedly enhanced in the TG surface-treated condition at 24 hours (2,625 ± 21.89 kΩ) and 144 hours (1,800 ± 10.54 kΩ) but is reduced

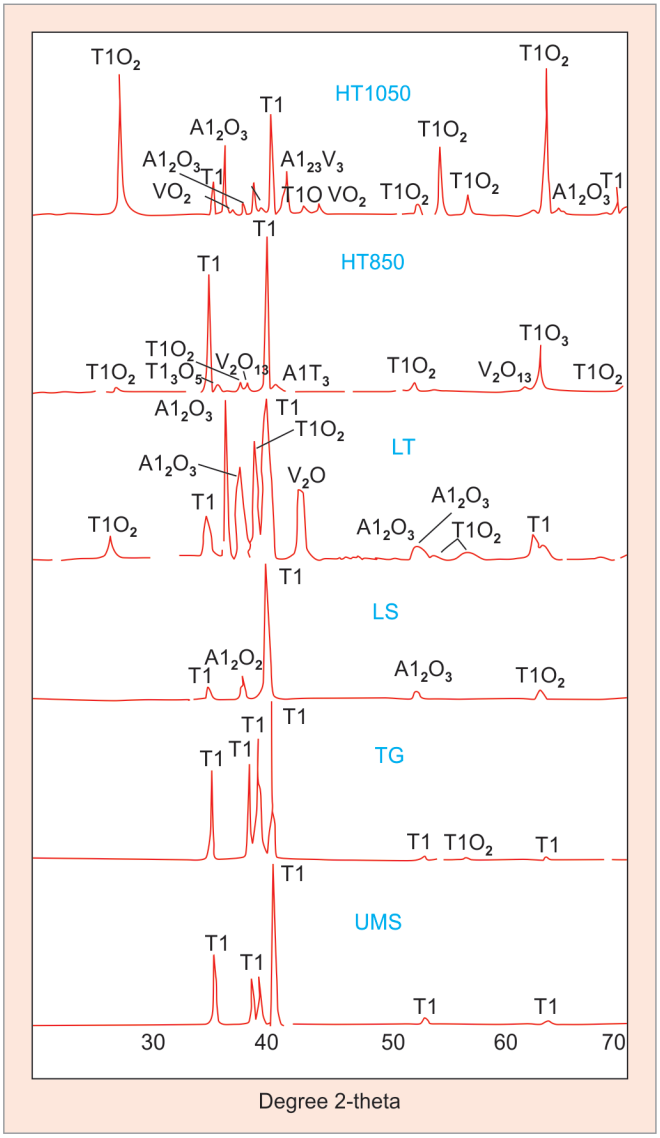

Fig. 3: X-ray diffraction patterns of the alloy Ti-6Al-4V, in unmodified and different surface-modified conditions

Table 1: Mean comparison of polarization resistance (R_p measured in kΩ) between 24 hours and 144 hours duration of exposure in simulated body fluid solution of various groups

	24 hours		*144 hours*			
Groups	*Mean*	*SD*	*Mean*	*SD*	*Mean ± SD difference*	*p value*
UMS	627.00	5.37	1,249.00	11.25	622.00 ± 5.88	0.000 S
HA	625.00	7.07	1,250.50	8.64	625.50 ± 1.57	0.000 S
LS	40.00	8.16	60.00	18.26	20.00 ± 10.10	0.012 S
LT	750.00	10.54	127.00	5.37	623.00 ± 5.17	0.000 S
TG	2,627.50	21.89	1,800.00	10.54	827.50 ± 11.35	0.000 S
HT850	260.00	17.64	780.00	11.55	520.00 ± 6.09	0.000 S
HT1050	0.00	0.00	0.00	0.00	0.00 ± 0.00	1.000 NS
p value	0.000 S		0.000 S			

S, significant at 0.05 level; NS, not significant

in the other surface-modified conditions. The LT samples showed enhanced R_p, i.e., (750 ± 10.54 kΩ) concerning UMS (627 ± 5.37 kΩ) and HA (625 ± 7.07 kΩ) initially (24 hours), but later (144 hours) markedly dropped (127 ± 5.37 kΩ) closest to LS samples (60 ± 18.26 kΩ), which is second-lowest corrosion-resistant among all surface modifications referred above. Interestingly, R_p was enhanced at 144 hours in both UMS (1,249 ± 11.25 kΩ) and HA (1,250 ± 8.65 kΩ) samples but was lower to TG (1,800 ± 10.54 kΩ). R_p may be seen to be least at both 24 and 144 hours (0.00 ± 0.00 kΩ) in the HT1050 condition. R_p is known to be an important parameter to characterize corrosion resistance of materials; the higher the value of R_p betters the corrosion resistance.

The above values suggest that corrosion resistance was markedly improved in TG concerning UMS (control group). On the contrary, corrosion resistance of the other surface-modified samples HA, LT, LS, HT850, and HT1050 was found to be reduced as compared to that of the UMS. Corrosion resistance was lowest in HT1050 conditions.

Multiple mean difference comparison of R_p between 24 hours and 144 hours duration of exposure in SBF solution of various groups is shown in Table 2. On statistical analysis using Tukey HSD test, the mean difference was significant ($p = 0.00$) among all groups both at 24 and 144 hours except between UMS and HA (2.00, $p = 1.000$) and (1.50, $p = 1.000$), respectively, at both the time periods indicating that there was no significant variation in the corrosion behavior of unmodified and HA-coated samples with time.

During CPT along with the continuous scanning potential, the current response was monitored. According to ASTM (F2129, G61) standards,[31,32] there are three different states:

- The scanning potential continues until the hysteresis loop is completed indicating repassivation.
- Oxygen evolution occurs and the anodic to cathodic transition potential is reached.
- The hysteresis loop is not completed and corrosion potential is reached.

The representative cyclic polarization curves obtained in SBF in the present study are shown in Figure 2 and all the groups represent the typical representative curve exhibiting apparent repassivation. The curves show forward and backward scans for the different surface-modified conditions along with that of the unmodified sample. In the case of TG (shown in Figure 2D), retracing of forward scan and backward scan resulted in the absence of a hysteresis loop indicating that the localized corrosion has not occurred. Positive loops concerning UMS, HA, LS, LT, HT850, and HT1050 as seen in Figure 2 show the greater probability of localized corrosion.

Pitting potential (E_{pit}), repassivation or protection potential (E_{rp}), the potential of anodic to cathodic transition, hysteresis, and active-passive transition (anodic nose) are the parameters used to interpret the cyclic polarization curves.[33] E_{corr} (mean corrosion potential), E_{pit}, E_{rp}, hysteresis, and E_{pit}-E_{rp} (amount of hysteresis) of all the groups which were determined through CPTs is graphically shown in Figure 4. For the relative position of E_{pit} and E_{rp}, the higher resistance against pitting the lower would be E_{pit}- E_{rp}. E_{pit}-E_{rp} was lowest in TG (0.00 ± 0.00 mV), gradually increased concerning LS (198.00 ± 54.53 mV), HA (262.50 ± 53.20 mV), LT (342.0 ± 0.50.56 mV), HT850 (507.0 ± 129.62 mV), UMS (534.50 ± 61.75 mV), and is highest in HT1050 (1,469.0 ± 49.54 mV). The data suggested that E_{pit}-E_{rp} of all groups TG, HA, LS, LT, and HT850 was lower than UMS (control) except HT1050. This suggests that all the surface modifications have lower susceptibility to localized corrosion (pitting and crevice

Table 2: Multiple mean difference comparison of polarization resistance (R_p measured in kΩ) between 24 hours and 144 hours duration of exposure in simulated body fluid solution of various groups

		UMS	*HA*	*LS*	*LT*	*TG*	*HT850*	*HT1050*
Groups	*Duration*	*Δ, p value*	*Δ, p value*	*Δ, p value*	*Δ, p value*	*Δ, p value*	*Δ, p value*	*Δ, p value*
UMS	24 hours	–	2.00, $p = 1.000$	587.00, $p = 0.000$*	123.00, $p = 0.000$*	2,000.50, $p = 0.000$*	367.00, $p = 0.000$*	627.00, $p = 0.000$*
	144 hours	–	1.50, $p = 1.000$	1,189.00, $p = 0.000$*	1,122.00, $p = 0.000$*	551.00, $p = 0.000$*	469.00, $p = 0.000$*	1,249.00, $p = 0.000$*
HA	24 hours	2.00, $p = 1.000$	–	585.00, $p = 0.000$*	125.00, $p = 0.000$*	2,002.50, $p = 0.000$*	365.00, $p = 0.000$*	625.00, $p = 0.000$*
	144 hours	1.50, $p = 1.000$	–	1,190.50, $p = 0.000$*	1,123.50, $p = 0.000$*	549.50, $p = 0.000$*	470.50, $p = 0.000$*	1,250.50, $p = 0.000$*
LS	24 hours	587.00, $p = 0.000$*	585.00, $p = 0.000$*	–	710.00, $p = 0.000$*	2,587.50, $p = 0.000$*	220.00, $p = 0.000$*	40.00, $p = 0.000$*
	144 hours	1,189.00, $p = 0.000$*	1,190.50, $p = 0.000$*	–	67.00, $p = 0.000$*	1,740.00, $p = 0.000$*	720.00, $p = 0.000$*	60.00, $p = 0.000$*
LT	24 hours	123.00, $p = 0.000$*	125.00, $p = 0.000$*	710.00, $p = 0.000$*	–	1,877.50, $p = 0.000$*	490.00, $p = 0.000$*	750.00, $p = 0.000$*
	144 hours	1,122.00, $p = 0.000$*	1,123.50, $p = 0.000$*	67.00, $p = 0.000$*	–	1,673.00, $p = 0.000$*	653.00, $p = 0.000$*	127.00, $p = 0.000$*
TG	24 hours	2,000.50, $p = 0.000$*	2,002.50, $p = 0.000$*	2,587.50, $p = 0.000$*	1,877.50, $p = 0.000$*	–	2,367.50, $p = 0.000$*	2,627.50, $p = 0.000$*
	144 hours	551.00, $p = 0.000$*	549.50, $p = 0.000$*	1,740.00, $p = 0.000$*	1,673.00, $p = 0.000$*	–	1,020.00, $p = 0.000$*	1,800.00, $p = 0.000$*
HT850	24 hours	367.00, $p = 0.000$*	365.00, $p = 0.000$*	220.00, $p = 0.000$*	490.00, $p = 0.000$*	2,367.50, $p = 0.000$*	–	260.00, $p = 0.000$*
	144 hours	469.00, $p = 0.000$*	470.50, $p = 0.000$*	720.00, $p = 0.000$*	653.00, $p = 0.000$*	1,020.00, $p = 0.000$*	–	780.00, $p = 0.000$*
HT1050	24 hours	627.00, $p = 0.000$*	625.00, $p = 0.000$*	40.00, $p = 0.000$*	750.00, $p = 0.000$*	2,627.50, $p = 0.000$*	260.00, $p = 0.000$*	–
	144 hours	1,249.00, $p = 0.000$*	1,250.50, $p = 0.000$*	60.00, $p = 0.000$*	127.00, $p = 0.000$*	1,800.00, $p = 0.000$*	780.00, $p = 0.000$*	–

Δ: Mean difference
*The mean difference is significant at the 0.05 level

corrosion) than unmodified surface alloy Ti-6Al-4V varying degrees except HT1050.

Comparison of E_{pit}-E_{rep} (amount of hysteresis) of mean differences between the various groups is shown in Table 3. On statistical analysis using Tukey HSD test ($p = 0.05$), the mean difference was statistically significant ($p = 0.00$) between all the groups except between UMS and HT850 (27.50, $p = 0.968$); between HA and LS (66.50, $p = 0.300$); and between HA and LS (77.50, $p = 0.148$). It indicates that there was no significant difference in the probability of localized corrosion was between UMS and HT850 and between HA, LS, and LT.

Discussion

As stated by Eliaz,[34] the corrosion resistance of an implant material affects its functionality and durability; it is a primary factor governing biocompatibility. Implantation may lead to hypersensitivity and cancer due to the exposure of fluctuating temperature and body fluids, despite the implant showing good clinical performance. Intraorally, partial dental frameworks and dental implants are exposed to saliva and varying acidic and alkaline conditions. Hence, understanding the corrosion behavior of dental implants in specific environments is very essential.

In vitro evaluation of localized corrosion, such as, pitting corrosion, crevice corrosion, and stress corrosion cracking of the metallic biomaterials can be evaluated using cyclic polarization techniques.[35] In the present study, Electrochemical impedance spectroscopy test and CPTs were carried for all the groups using GAMRY Potentiostat following the instructions by ASTM standards.[28] Polarization resistance (R_p) is known to be an important parameter to characterize corrosion resistance of materials derived from the EIS test; higher the value of R_p betters the corrosion resistance. In the present study, corrosion resistance was markedly improved in TG concerning UMS (control group). On the contrary, corrosion resistance of the other surface-modified groups HA, LS, LT, HT850, and HT1050, was found to be reduced as compared to that of the UMS. Corrosion resistance was lowest in the HT1050 conditions.

Silverman stated that pitting potential (E_{pit}), repassivation or protection potential (E_{rp}), the potential of anodic to cathodic transition, hysteresis, and active-passive transition (anodic nose) are

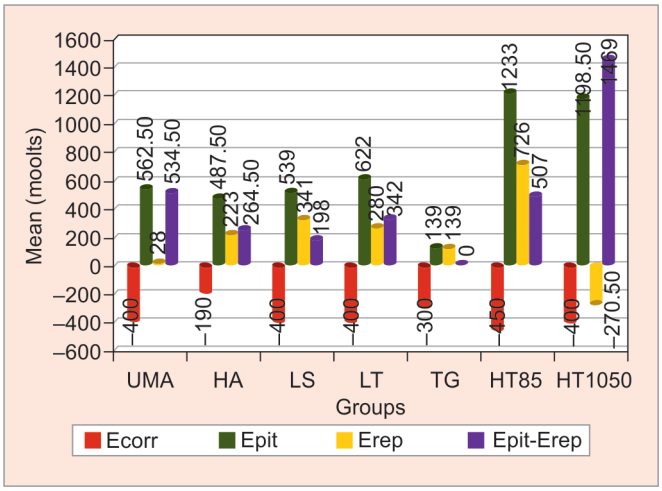

Fig. 4: Graph showing mean corrosion potential (E_{corr}), pitting potential (E_{pit}), and repassivation or protection potential (E_{rp}), and amount of hysteresis (E_{pit}-E_{rp}) of the various groups determined through cyclic polarization tests

Table 3: Mean difference comparison of E_{pit}-E_{rp} (amount of hysteresis) between the various groups

	UMS	*HA*	*LS*	*LT*	*TG*	*HT850*	*HT1050*
Groups	*Δ, p value*	*Δ, p value*	*Δ, p value*	*Δ, p value*	*Δ, p value*	*Δ, p value*	*Δ, p value*
UMS	–	270.00, $p = 0.000$*	336.50, $p = 0.000$*	192.50, $p = 0.000$*	534.50, $p = 0.000$*	27.50, $p = 0.968$	934.50, $p = 0.000$*
HA	270.00, $p = 0.000$*	–	66.50, $p = 0.300$	77.50, $p = 0.148$	264.50, $p = 0.000$*	242.50, $p = 0.000$*	1,204.50, $p = 0.000$*
LS	336.50, $p = 0.000$*	66.50, $p = 0.300$	–	144.00, $p = 0.000$*	198.00, $p = 0.000$*	309.00, $p = 0.000$*	1,271.00, $p = 0.000$*
LT	192.50, $p = 0.000$*	77.50, $p = 0.148$	144.00, $p = 0.000$*	–	342.00, $p = 0.000$*	165.00, $p = 0.000$*	1,127.00, $p = 0.000$*
TG	534.50, $p = 0.000$*	264.50, $p = 0.000$*	198.00, $p = 0.000$*	342.00, $p = 0.000$*	–	507.00, $p = 0.000$*	1,469.00, $p = 0.000$*
HT850	27.50, $p = 0.968$	242.50, $p = 0.000$*	309.00, $p = 0.000$*	165.00, $p = 0.000$*	507.00, $p = 0.000$*	–	962.00, $p = 0.000$*
HT1050	934.50, $p = 0.000$*	1,204.50, $p = 0.000$*	1,271.00, $p = 0.000$*	1,127.00, $p = 0.000$*	1,469.00, $p = 0.000$*	962.00, $p = 0.000$*	–

Δ: Mean difference
*The mean difference is significant at the 0.05 level

the parameters used to interpret the cyclic polarization curves.[33] The more difference between the E_{pit} and E_{rp} and the larger area of a positive loop (hysteresis) demonstrating the probability of low pitting corrosion resistance.[28]

The relative position of pitting potential and repassivation potential or protective potential concerning the corrosion potential are the most important parameters for evaluating the pitting corrosion behavior.[36] In the polarization curve, the scanning direction changes at pitting potential as a forward curve, scanning continues until the reverse curve crosses the forward polarization curve and this intersection point is named protection potential. Pitting potential is the minimum potential at which the material tends to the pitting corrosion. Above the pitting potential, new pits will initiate and develop.[37] Repassivation potential is the potential at which the growth rate of pits is stopped.

The occurrence of hysteresis in the curve is when the forward curve is not overlaid with the reverse scanning curve. The difference between forward and reverse current density at the same potential demonstrates the size of hysteresis. The amount of hysteresis or in the other words, the difference between E_{pit}-E_{rp} indicates the amount of localized corrosion.[38] The difference between the E_{pit} and E_{rp} and also the area of the hysteresis loop indicate the probability of localized corrosion.

The representative cyclic polarization curves of all the groups obtained in SBF in the present study are shown in Figure 2. It may be seen that there is a wide variation in the protection potential and the area of the hysteresis loops. The absence of a hysteresis loop during the potential scan (the forward curve coincides with the reverse curve) indicates that there was no occurrence of the localized corrosion[39,40] which is seen in the case of TG. Positive loops concerning UMS, HA, LS, LT, HT850, and HT1050 show a decrease in passivity due to localized corrosion (pitting and crevice corrosion).

However, it is important to understand the present *in vitro* study results have to be applied cautiously as it differs from *in vivo* tests. *In vitro* and *in vivo* corrosion data were reviewed by Kuhn et al.[41] and concluded that the use of electrochemical techniques conducted in simple electrolytes affords a valid means of ranking or screening biomaterials.

Revie and Uhlig[42] summarized the characteristics of surface oxide film on various metallic biomaterials. Commercially pure Ti surface oxides constitute Ti0, Ti2+, and Ti3+ and Ti4+. Ti-6Al-4V alloy surface consisted of TiO_2, Al_2O_3, hydroxyl groups, and bound water. The alloying element V was not detected. These findings matched the surface oxides of UMS group of our study.

It may be seen that while there was the only presence of TiO_2 in the TG sample, there was TiO_2 as well as Al_2O_3 in the LS condition. X-ray diffraction analysis found the formation of newer oxides [LASER textured (LS)—V_2O; oxidized state (HT850)—V_6O_{13} and $AlTi_3$; oxidized state (HT1050)—V_2O_5, VO_2, and oxidized state (HT1050)—V_2O_5, VO_2] in their respective modifications as compared with unmodified surface alloy of the present study. These newer oxides may be detrimental to the biocompatibility of the Ti-6Al-4V alloy which needs to be correlated with the results of corrosion tests.

Titanium and its alloys are the most widely used as medical implants as they are light, biologically, and chemically inert and have a low electrical and thermal conductivity in comparison to other metals. The modulus of elasticity of titanium and its alloys is closer to that of bone than the moduli of stainless steels and cobalt-based alloys, thus reducing the occurrence of stress shielding after implantation. Minimal image interferences are seen in magnetic resonance imaging (MRI) or computed tomography (CT) scans due to their weak paramagnetism. Their coefficient of thermal expansion is similar to that of bone, thus minimizing the distortion of MRI images. The formation of a thick oxide layer on the surface of titanium and its alloys is due to their high affinity to oxygen, providing corrosion resistance and histological osseointegration. This oxide layer is thermodynamically stable and found to repassivate.[3]

Ti-6Al-4V used in the present study is the most common alloy used in medicine.[27] It combines good workability, heat treatment ability, and weldability, as well as high corrosion resistance, high strength, and biocompatibility.

In the present study, on optical microscopic evaluation of the Ti-6Al-4V alloy showed a dual microstructure (Fig. 1), which consisted of mainly fine-grained hcp (α) phase distributed in bcc (β) phase indicating higher strength and corrosion resistance. The presence of elements, such as, Al, O, N, Ga, and C was found to stabilize the phase, whereas metals, such as, V, Nb, Ta, and Mo stabilized the β phase. The microstructure and mechanical properties of Ti-6Al-4V are greatly dependent on the thermomechanical processing treatments. If the material is cooled too slowly, the β phase becomes more noticeable and lowers the strength and corrosion resistance of the alloy.[3]

Aksakal et al.[43] stated that leaching of the metallic ions *in vivo* due to corrosion leads to various biological effects. The biomaterial Ti-6Al-4V alloy showed leaching of aluminum (Al) causing epileptic effects and Alzheimer's disease; vanadium (V) was toxic in the elementary state. Asri et al.[44] stated that surface modifications may be considered as a "best solution" to enhance corrosion resistance; besides achieving superior biocompatibility and promoting osseointegration of biomaterials. Several surface modification techniques include deposition of the coating, development of passivating oxide layer and ion beam surface modification, and also surface texturing methods, such as, plasma spraying, chemical etching, blasting, electropolishing, and laser treatment. A systematic review by Wennerberg and Albrektsson stated that the titanium surface topography influenced bone response at the micrometer level.[45]

Queiroz et al.[46] assessed the surfaces of commercially pure titanium implants (cp Ti) with modified surfaces by a laser beam (LS); with and without hydroxyapatite (HA) deposition; without (HAB) and with (HABT) thermal treatment utilizing histomorphometric and descriptive histological analyzes in their *in vivo* study. It provided evidence that LS, HAB, and HABT-modified surfaces improved bone-to-implant contact and increased bone formation around osseointegrated implants compared to conventional machined implants favoring the osseointegration process. But, the R_p values of LASER sintering (LS) were found to be second-lowest in our study consisting of Ti-6Al-4V alloy which suggests lower biocompatibility; LASER texturing (LT) was closer to UMS (control) and HA.

Tian et al.[47] stated that lasers have the intrinsic properties of high coherence and directionality, as its beam can focus onto the metallic surface to perform a broad range of treatments, such as, remelting, alloying, and cladding, which are used to improve the wear and corrosion resistance of titanium alloys. del Pino et al.[48] performed surface oxidation of titanium by irradiation in the air with an Nd:YAG (λ = 1.064 μm) laser operating in pulsed mode and reported that their compositional studies performed by XRD showed that the coatings were mainly composed of Ti_2O and TiO which are similar to our study. Excimer laser surface treatment of Ti-6Al-4V alloy was done by Yue et al.[49] to improve the pitting corrosion resistance of the alloy. The electrochemical behaviors of

the untreated and the laser-treated specimens were evaluated by electrochemical polarization tests. Excimer laser surface treatment significantly increased the pitting potential of the Ti alloy, especially when the material was treated in argon gas.

In the present study, an attempt was made to evaluate and compare chemical, thermal, and lasers surface modifications on the same experimental setup and to understand the corrosion behavior of surface-modified Ti-6Al-4V alloy along with the unmodified surface. It is obvious that while in the HA sample there is hydroxyapatite, a biomaterial, and there are TiO_2 and Al_2O_3 in LASER sintered (LS) and combined chemical and thermal treated (TG)—TiO_2 surface-treated conditions. The TiO_2 and Al_2O_3 oxides are known to be bio-inert[50] materials. TG, HA, and LS oxides are suggestive of good osseointegration but when correlated with the results of corrosion tests, LS shows less R_p indicating less corrosion resistance.

Hydrogen peroxide (H_2O_2) is found to be an oxidizing molecule, which is secreted by cells and is associated with wound healing and is thus present in significant quantities in fresh implant environments. Also, the highest corrosion resistance of the TG sample [surface treatment consisted of soaking of the sample in a 6% (by mass) hydrogen peroxide solution at 60°C for 4 hours and subsequent heating at 400°C for 1 hour, followed by furnace cooling] may be attributed to the formation of a thin, compact, and adherent film of titania gel (TiO_2) on its surface which match the results of studies done by Bearinger et al.[51,52] They studied the morphological changes of TiO_2 oxide films on CP-Ti and Ti-6Al-4V alloy; upon exposure to PBS and hydrogen peroxide-modified PBS solutions, all the samples were found covered with protective titanium oxide domes developed in that area.

Corrosion tests, a tool widely used to assess the self-passivating ability and resistance against pitting in all groups, showed enhanced polarization resistance (R_p) and low susceptibility to localized corrosion (retracing of forward and backward scan without the formation of hysteresis loop) in TG sample suggests its improved biocompatibility. Thus, the null hypothesis stating that the different surface modifications of implant grade Ti-6Al-4V alloy have no influence on its corrosion behavior is being rejected.

The study could not mimic the *in vivo* environment due to the high concentration of dissolved in O_2 in isotonic solutions as compared to venous blood which may lead to passivation. The circular flat disks samples used in the present *in vitro* study do not match the implant geometry which has threads for mechanical engagement in bone; size, shape, and surface wettability of the alloy are found to influence biocompatibility.

There is a need to evaluate the corrosion behavior of new Ti alloys without vanadium, such as, Ti–15Mo–3Nb, Ti–Mo–Nb–Al, Ti–Mo–Nb–Al–Cr–Zr, Ti–13Zr–13Nb, Ti–15Zr–4Nb, Ti–6Al–7Nb, Ti–Zr–Nb–Ta–Pd, Ti–Mo–Nb–Al, Ti–Mo–Nb–Al–Cr–Zr, Ti–Zr–Nb, and Ti–Zr–Nb–Ta–Pd. To assess the influence of fluoride ions, present in dental gels on the surface-modified layer of titanium alloy Ti-6Al-4V and the stability of the corrosion products formed.

Conclusion

- Combined chemical and thermal treated (TG) condition has highest corrosion resistance in comparison to unmodified titanium surfaces (UMS), whereas hydroxyapatite-coated, LASER-modified surfaces, oxidized states (850 and 1,050°C) are lower to UMS. Oxidized state at higher temperatures (1,050°C) was the lowest corrosion-resistant surface.
- Surface modifications have enhanced the resistance against localized corrosion in TG followed by HA, LS, LT, and HT850 than unmodified titanium surfaces (UMS) by increasing the surface passivity except in oxidized state at higher temperatures (1,050°C) within the limitations of the study.
- Combined chemical and thermal treatment of titanium alloy showed greater biocompatibility than the unmodified surface.

References

1. Williams DF, Black J, Doherty PJ. Consensus report of second conference on definitions in biomaterials. Biomaterial-Tissue Interfaces Doherty PJ, Williams RL, Williams DF, et al., ed., vol. 10, Amsterdam, The Netherlands: Elsevier; 1992. pp. 525–533.
2. Williams DF, ed. Definitions in biomaterials-Proceedings of a consensus conference of the European Society Biomaterials, vol. 4, New York, NY, USA: Elsevier; 1987.
3. Brunette DM, Tengvall P, Textor M, et al., ed. Titanium in medicine. Heidelberg, Germany: Springer; 2001.
4. Gilbert JL, Mali S. Medical implant corrosion: Electrochemistry at metallic biomaterial surfaces. In: Degradation of implant materials Eliaz N, ed., ch. 1, New York, NY, USA: Springer; 2012. pp. 1–28.
5. Gepreel MAH, Niinomi M. Biocompatibility of Ti-alloys for long-term implantation. J Mech Behav Biomed Mater 2013;20:407–415. DOI: 10.1016/j.jmbbm.2012.11.014.
6. Khan MA, Williams RL, Williams DF. The corrosion behaviour of Ti-6Al-4V, Ti-6Al-7Nb and Ti-13Nb-13Zr in protein solutions. Biomaterials 1999;20(7):631–637. DOI: 10.1016/S0142-9612(98)00217-8.
7. Khan MA, Williams RL, Williams DF. Conjoint corrosion and wear in titanium alloys. Biomaterials 1999;20(8):765–772. DOI: 10.1016/S0142-9612(98)00229-4.
8. Singh R, Dahotre NB. Corrosion degradation and prevention by surface modification of biometallic materials. J Mater Sci Mater Med 2007;18(5):725–751. DOI: 10.1007/s10856-006-0016-y.
9. Ducheyne P. In-vitro corrosion study of porous metal fibre coatings for bone ingrowth. Biomaterials 1983;4(3):185–191. DOI: 10.1016/0142-9612(83)90008-X.
10. Gotfredsen K, Wennerberg A, Johansson C, et al. Anchorage of TiCV blasted, HA-coated, and machined implants: an experimental study with rabbits. J Biomed Mater Res 1995;29(10):1223–1231. DOI: 10.1002/jbm.820291009.
11. Piattelli A, Manzon L, Scarano A, et al. Histologic and histomorphometric analysis of the bone response to machined and sand blasted titanium implants: an experimental study in rabbits. Int J Oral Maxillofac Implants 1998;13(6):805–810. DOI: 10.11607/prd.5139.
12. Lauer G, Wiedmann-Al-Ahmad M, Otten JE, et al. The titanium surface texture effects adherence and growth of human gingival keratinocytes and human maxillary osteoblast-like cells in vitro. Biomaterials 2001;22(20):2799–2809. DOI: 10.1016/S0142-9612(01)00024-2.
13. Li D, Liu B, Wu J, et al. Bone interface of dental implants cytologically influenced by a modified sandblasted surface: a preliminary in vitro study. Implant Dent 2001;10(2):132–138. DOI: 10.1097/00008505-200104000-00010.
14. Di Carmine M, Toto P, Feliciani C, et al. Spreading of epithelial cells on machined and sandblasted titanium surfaces: an in-vitro study. J Periodontal 2003;74(3):289–295. DOI: 10.1902/jop.2003.74.3.289.
15. Zreiqat H, Akin FA, Howlett CR, et al. Differentiation of human bone-derived cells grown on GRGDSP-peptide bound titanium surfaces. J Biomed Mater Res 2003;64(1):105–113. DOI: 10.1002/jbm.a.10376.
16. Garcia-Alonso MC, Saldana L, Valles G, et al. In vitro corrosion behaviour and osteoblast response of thermally oxidized

Ti6Al4V alloy. Biomaterials 2003;24(1):19–26. DOI: 10.1016/S0142-9612(02)00237-5.
17. Laing PG. Compatibility of biomaterials. Orthop Clin North Am 1973;4:249–273.
18. Sarkar NK, Marshall GW, Reener EH. In-vivo and in-vitro corrosion products of dental amalgam. J Dental Res 1975;54(5):1031–1038. DOI: 10.1177/00220345750540050501.
19. Sarkar NK, Fuys RA, Stanford JW. The chloride corrosion of low-gold casting alloys. J Dental Res 1979;58(2):568–575. DOI: 10.1177/00220345790580020501.
20. Strub JR, Eyer CS, Sarkar NK. Heat treatment, microstructure and corrosion of low-gold casting alloy. J Oral Rehabilitation 1986;13(6):521–528. DOI: 10.1111/j.1365-2842.1986.tb00675.x.
21. Lemaitre L, Moors M, Vanpeteghem AP. A mechanistic study of the electrochemical corrosion of the gamma2 phase in dental amalgams: evaluation of the measurements. J Oral Rehabil 1989;16(6):537–542. DOI: 10.1111/j.1365-2842.1989.tb01375.x.
22. Chern Lin JH, Moser JB, Taira M, et al. Co-Ti and Ni-Ti systems: corrosion and micro hardness. J Oral Rehabil 1990;17(4):383–393. DOI: 10.1111/j.1365-2842.1990.tb00023.x.
23. Mueller HJ. Tarnish and corrosion of dental alloys. Metal handbook, vol. 13, Corrosion 9th ed., Metals Park, OH: ASM Int; 1987. pp 1336–1366.
24. Kokubo T, Ito S, Huang ZT, et al. Solutions able to reproduce in vivo surface-structure changes in bioactive glass-ceramic A-W[3]. Bio Mater Res 1990;24(6):721–734. DOI: 10.1002/jbm.820240607.
25. Filgueriras MR, Torre GL, Hench LL. Solution effects on the surface reaction of a bioactive glass. J Bio Mater Res 1993;27(4):445–453. DOI: 10.1002/jbm.820270405.
26. Kim HM, Kishimoto K, Miyaji F, et al. Composition and structure of the apatite formed on PET substrates in SBF modified with various ionic activity products. J Mater Sci Mater Med 2000;11(7):421–426. DOI: 10.1023/A:1008935924847.
27. Implants for Surgery—Metallic Materials—Part 3: Wrought Titanium 6-Aluminium 4-Vanadium Alloy; ISO5832-3:2016; International Organization for Standardization: Geneva, Switzerland, 2016.
28. Mc Cafferty E. Introduction to corrosion science. NewYork: Springer; 2010.
29. Scully JR. Polarization resistance method for determination of instantaneous corrosion rates. Corrosion 2000;56(2):199–218. DOI: 10.5006/1.3280536.
30. ASTM. G106.89: practice for verification of algorithm and equipment for electrochemical impedance measurements. Annual Book of ASTM Standards, vol. 03, issue 02, West Conshohocken, PA: ASTM Int; 2015.
31. ASTM G61.68: Standard Test Method, West Conshohocken, PA: ASTM Int., 2014.
32. ASTM F2129.15: Standard Test Method, West Conshohocken, PA: ASTM Int., 2015.
33. Silverman DC. Practical corrosion prediction using electrochemical techniques. John Wiley and Sons; 2011.
34. Eliaz N. Corrosion of metallic biomaterials: a review. Materials 2019;12(3):407. DOI: 10.3390/ma12030407.
35. Esmailzadeh S, Aliofkhazraei M, Sarlak H. Interpretation of cyclic potentiodynamic polarization test results for study of corrosion behavior of metals: a review. Protect Met Physi Chemis Surf 2018;54(5):976–989. DOI: 10.1134/S207020511805026X.
36. Wang B, Liu J, Yin M, et al. Comparison of corrosion behavior of Al-Mn and Al-Mg alloys in chloride aqueous solution. Mater Corros 2016;67(1):51–59. DOI: 10.1002/maco.201408211.
37. Khamaj JA. Cyclic polarization analysis of corrosion behavior of ceramic coating on 6061 Al/SiCp composite for marine applications. Prot Met Phys Chem Surf 2016;52(5):886–889. DOI: 10.1134/S2070205116050117.
38. Kelly RG, Scully JR, Shoesmith D, et al. Electrochemical techniques in corrosion science and engineering. New York: CRC Press; 2002.
39. Silverman DC. Tutorial on cyclic potentiodynamic polarization technique. Corrosion 1998;1:21.
40. Li L, Qu Q, Bai W, et al. Effect of NaCl on the corrosion of cold rolled steel in peracetic acid solution. Int J Electrochem Sci 2012;7(4):3773.
41. Kuhn AT, Neufeld P, Rae T. Synthetic environments for testing of metallic biomaterials. The use of synthetic environments for corrosion testing, ASTM STP 970. Francis PE, Lee TS, ed., Philadelphia, PA, USA: ASTM; 1988. pp. 79–95.
42. Revie R, Uhlig HH. Corrosion and corrosion control: An introduction to corrosion science and engineering. 4th ed., Hoboken, NJ, USA: John Wiley & Sons; 2008. p. 84.
43. Aksakal B, Yildirim ÖS, Gul H. Metallurgical failure analysis of various implant materials used in orthopedic applications. J Fail Anal Prev 2004;4(3):17–23. DOI: 10.1007/s11668-996-0007-9.
44. Asri RIM, Harun WSW, Samykano M, et al. Corrosion and surface modification on biocompatible metals: a review. Mater Sci Eng C Mater Biol Appl 2017;77(1):1261–1274. DOI: 10.1016/j.msec.2017.04.102.
45. Wennerberg A, Albrektsson T. Effects of titanium surface topography on bone integration: a systematic review. Clinic Oral Implants Res 2009;20:172–184. DOI: 10.1111/j.1600-0501.2009.01775.x.
46. Queiroz TP, de Molon RS, Souza FÁ, et al. In vivo evaluation of cp Ti implants with modified surfaces by laser beam with and without hydroxyapatite chemical deposition and without and with thermal treatment: topographic characterization and histomorphometric analysis in rabbits. Clin Oral Invest 2017;21(2):685–699. DOI: 10.1007/s00784-016-1936-7.
47. TianY ChenC, Li S, Huo Q. Research progress on laser surface modification of titanium alloys. Appl Surf Sci 2005;242(1-2):177–184. DOI: 10.1016/j.apsusc.2004.08.011.
48. del Pino AP, Serra P, Morenza J. Oxidation of titanium through Nd: YAG laser irradiation. Appl Sur Sci 2002;197:887–890. DOI: 10.1016/S0169-4332(02)00447-6.
49. Yue T, Yu J, MeiZ, et al. Excimer laser surface treatment of Ti–6Al–4V alloy for corrosion resistance enhancement. Mater Lett 2002;52(3):206–212. DOI: 10.1016/S0167-577X(01)00395-0.
50. Spiekermann H. Implantology, in color atlas of dental medicine Rateitschak KH Wolf HF, ed., New York: THIEME Medical Publishers Inc; 1995. pp. 12–16.
51. Bearinger JP, The Electrochemistry of titanium/titanium oxide in the biological environment. Ph.D. thesis, Northwestern University, Evanston, IL, USA, 2000.
52. BearingerJP OrmecCA, Gilbert JL. In situ imaging and impedance measurements of titanium surfaces using AFM and SPIS. Biomaterials 2003;24(11):1837–1852. DOI: 10.1016/S0142-9612(02)00547-1.